LAWRENCE
LIVERMORE
NATIONAL
LABORATORY

LLNL-JRNL-850317

Approaching to Melt-castable 3,4-Bis(3-(4-nitro-1,2,5-oxadiazol-3-yl)-1,2,4-oxadiazol-5-(LLM-210): Design, Synthesis, and Characterization

M. X. Zhang, P. F. Pagoria, A. J. DeHope, I. W. Kuo, D. A. Parrish

June 14, 2023

New Journal of Chemistry

Disclaimer

Oxadiazole-based Heterocycles as Building Block for Material Property Control: Design, Synthesis, and Characterization of 3,4-Bis(3-(4-nitro-1,2,5-oxadiazol-3-yl)-1,2,4-oxadiazol-5-yl)-1,2,5-oxadiazole (**LLM-210**)

Mao-Xi Zhang,*† Philip F. Pagoria,† Alan J. DeHope,† I-Feng W. Kuo, *† Andrew T. Kerr, ‡ and Damon A. Parrish‡

ABSTRACT

This paper presents an approach to novel oxadiazole-based melt-castable energetic material, **LLM-210**. Used in pour-in process and 3D printing, melt-castable energetic materials (MCEM) must possess required physical and safety properties of industry-standard energetic materials, also a narrow range of melting point between 80-100 °C. Melting point is difficult to accurately predict, therefore, searching for MCEM is challenging. 3,4-Bis(5-(4-nitro-1,2,5-oxadiazol-3-yl)-1,2,4-oxadiazol-3-yl)-1,2,5-oxadiazole (**LLM-205**), composed of five-oxadiazole rings allied *via* carbon-carbon bonds, was selected as new MCEM candidate. The target molecule was synthesized and characterized, showing a density of 1.807g/cm^3; thermal decomposing temperature at 299 °C; and insensitive to external stimuli, but the melting point of 104 °C was out of the rang. Based on the molecular properties and *ab initio* calculations, 3,4-bis(3-(4-nitro-1,2,5-oxadiazol-3-yl)-1,2,4-oxadiazol-5-yl)-1,2,5-oxadiazole (**LLM-210**), an isomer of **LLM-205**, was designed and synthesized from a different way. **LLM-210** was characterized as MCEM, possessing melting point of 87 °C; density of 1.812 g/cm^3; and exothermally decomposing temperature at 314 °C; being insensitive to external stimuli. In this paper, the relationship of molecular structure to properties of **LLM-205** and **LLM-210** based on the results of Density Functional Theory (DFT) and X-ray crystallographic analysis is also briefly discussed.

Key words: heterocycle, oxadiazole, explosive, melt-castable

Introduction

In recent years, melt-castable energetic materials (MCEM) have attracted significant attention in energetic material research due to the applications in pour-in process and 3D printing.[1-3] The development of novel MCEMs is a difficult task because the stringent requirements needed for a viable material. New MCEM must possess high thermal stability and low sensitivity to external stimuli in both solid and molten state and have a narrow melting point range of 80 - 100 °C. The narrow range of temperature is required so that the material can be molten using legacy steam equipment for casting operations. In the past decades many melt-castable energetic materials were designed and synthesized, but few possesses the combination of thermal stability, density, sensitivity, and performance superior to 2,4,6-trinitrotoulene (TNT) to make them viable alternatives.[2] TNT is a traditional melt-pour energetic material used worldwide in the military and civilian industry today. The material has melting point of 80 °C, decomposes exothermally at 295 °C, and resists insensitively to external stimuli. However, the performance of TNT is relatively low due to a negative heat of formation (-15 kcal/mol) and a relatively low density (ρ = 1.65 g/cm^3).[4, 5] The other drawback is that TNT and its post-detonation residues have been found to be environmentally persistent, polluting both soil and underground aquifers.[6, 7] Therefore, development of novel, more powerful, and environmentally friendly MCEMs has become an important task in energetic material research community.

Melting point, performance, and safety are among the critical parameters in design and synthesis of new MCEMs. Due to the narrow range of the melting point required plus the lack of accurate melting point predictive methods, a common strategy in the development of new MCEM is to introduce commonly known functional groups with historical precedence to lower melting points, such as, methyl (-Me), nitrate (-CH_2-O-NO_2), azido (-CH_2-N_3), nitramino (-N-NO_2), methylamino (-N-CH_3), or trinitromethyl (-$C(NO_2)_3$, etc. into core energetic components to adjust melting point while maintaining high performance.[2] But these modifications often result in decreasing density, or thermostability, or increase sensitivity. Oxadiazoles, including 1,2,4-, 1,2,5-, and 1,3,4-oxadiazole, are natural friendly heterocycles,[8, 9] having received considerable interest as building blocks in the synthesis of multi-cyclic energetic compounds because their incorporation often produce target compounds with high thermal stability, high density, positive heat of formation, and low sensitivity.[10-14] Previously, we reported the design and synthesis of several oxadiazole-based energetic compounds, 3,4-di(4-nitro-1,2,5-oxadiazolyl-3)-1,2,5-oxadiazole (**LLM-172**), 4''-nitro-[3,3':4',3''-ter(1,2,5-oxadiazol)]-4-amine (**LLM-175**), 3,5-di(4-nitro-1,2,5-oxadiazolyl-3)-1,2,4-oxadiazole (**LLM-191**), 4-(3-(4-nitro-1,2,5-oxadiazol-3-yl)-1,2,4-oxadiazol-5-yl)-1,2,5-oxadiazol-3-amine (**LLM-192**), 3,3'-bis(4-nitro-1,2,5-oxadiazol-3-yl)-5,5'-bi(1,2,4-oxadiazole) (**LLM-200**), and 3-(4-nitro-1,2,5-oxadiazol-3-yl)-1,2,4-oxadiazol-5-amine (**LLM-201**).[5,13,15-17] revealed that these oxadiazole-based energetic materials are

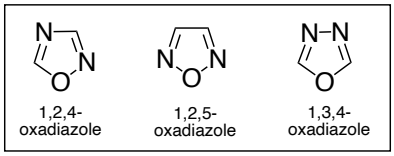

†Lawrence Livermore National Laboratory, 7000 East Ave, Livermore, California 94550, United States.
email: zhang27@llnl.gov, kuo2@llnl.gov
‡ Naval Research Laboratory, 4555 Overlook Ave, Washington DC 20375, United State

Electronic supplementary information (ESI) available. CCDC 2281441, 2281442, 2281443. For ESI and NMR, IR, crystallographic data see DOI: XXXXX

thermally stability (exothermal decomposition, T_d > 250 °C), high density (ρ > 1.70 g/cm^3), and low sensitivity (Dh_{50} > 32 cm, 1,3,5,7-tetranitro-1,3,5,7-tetrazocane, HMX). Among the molecules, **LLM-172, LLM-175, LLM-192,** and **LLM-201** are melt-castable energetic materials that indeed possess desirable properties, but other properties are not fully satisfied. Therefore, we extended our research to other oxadiazole-based materials for a better MCEM.

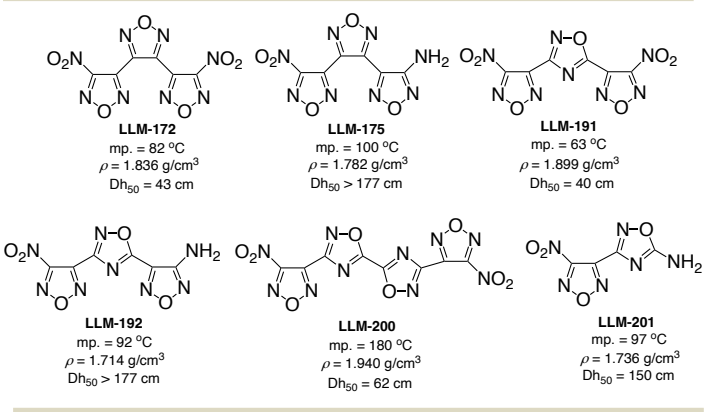

Taking the advantage of high density and relative low sensitivity to drop-weight impact testing, we anticipated that modifications to the core structure of **LLM-200** by inserting a 1,2,5-oxadiazole ring to the bond between the 1,2,4-oxadiazole rings to change a linear structure to V-type molecular shape would produce a material with a lower melting point while remaining desirable physical properties. Therefore, we designed and synthesized 3,4-bis(5-(4-nitro-1,2,5-oxadiazol-3-yl)-1,2,4-oxadiazol-3-yl)-1,2,5-oxadiazole (**LLM-205**), a V-type molecule composed of five oxadiazole units. Indeed, the melting point of **LLM-205** was significantly decreased but still at the edge of MCEM threshold. Based on the results and *ab initio* calculations, we modified the molecular structure by changing the connectivity of 1,2,4-oxadiazole rings. This modification led to the formation of title molecule 3,4-bis(3-(4-nitro-1,2,5-oxadiazol-3-yl)-1,2,4-oxadiazol-5-yl)-1,2,5-oxadiazole (**LLM-210**). In this paper, we report the design, synthesis, and characterization of **LLM-205** and **LLM-210** and discuss the properties of the materials based on the results of Density Functional Theory (DFT) and X-ray crystallographic analysis.

Results and Discussion

*Design and synthesis of **LLM-205** and **LLM-210***

LLM-205 contains five oxadiazole units, in which two 1,2,4-oxadiazoles, each carrying a nitro-1,2,5-oxadiazole ring, symmetrically attached to central 1,2,5-oxadiazole (furazan). Several methods can be used to prepare the material, but the most practical and convenient approach is to build 1,2,4-oxadiazole rings to bridge the furazans because condensing amidoxime and nitrile or ester is a common methodology for the preparation of 1,2,4-oxadiazole rings in organic synthesis.[16, 18-20] Thus, **LLM-205** was designed and synthesized by the oxidation of diamine (**6**) with hydrogen peroxide (Scheme 1). Compound **6** was obtained by condensing amidoxime (**4**) with nitrile (**5**) at elevated temperatures, in which **4** was prepared via a 3-step procedure involving the nitration of commercially available cyanoacetic acid (**1**) with HNO_3 in trifluoracetic acid (TFA) to give 3,4-dicyanofuroxan (**2**),[21] followed by deoxygenation with $P(OEt)_3$ to 3,4,-dicyanofurazan (**3**),[17, 22] and subsequent treatment with hydroxylamine.[23] Nitrile **5** was prepared by a modification of a published procedure by the oxidation the precursor amidoxime **11** (see Scheme 2) with lead acetate.[16]

Scheme 1

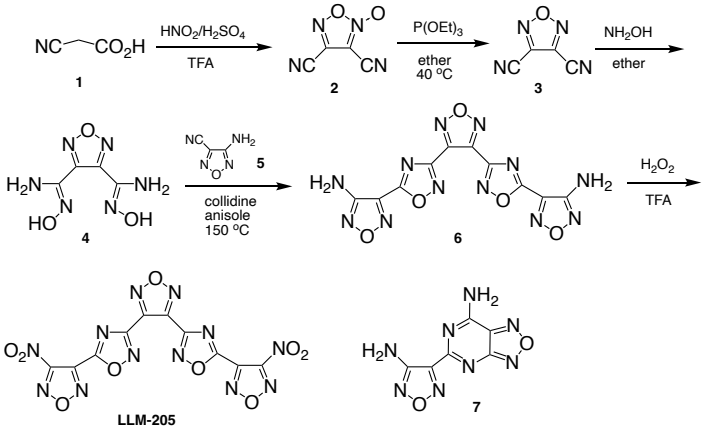

Diamine **6** was prepared according to our typical procedures by heating amidoxime **4** and nitrile **5** in the presence of catalytic collidine.[16] It was found that the yield of **6** depended on the ratio of the hindered base catalyst collidine to nitrile (**5**). When 3.5% of collidine was used, the condensation gave diamine in ~25% of yield. Increasing the ratio of collidine to 15% decreased the yield, but increased the yield of the byproduct 5-(4-amino-1,2,5-oxadiazol-3-yl)-[1,2,5]oxadiazolo[3,4-*d*]pyrimidin-7-amine (**7**), a dimer of nitrile (**5**).[16] The optimal conditions we found was the use of ~ 8% of collidine and heating the mixture in an anisole/toluene mixture at 165 °C while collecting the toluene-water azeotrope. Under the conditions, diamine **6** was isolated in 40-50% of yield.

The conversion of diamine **6** to **LLM-205** was carried out in TFA with aqueous H_2O_2 (70%) at room temperature. The yield was 30-40%, unoptimized. As expected, **LLM-205** is thermally stable, insensitive, and highly dense (*vide infra*), but the melting point (m.p. = 104 °C) is out of the range of malt-castable energetic material criteria. Therefore, attempts to lower the melting point by a modification of the molecular structure was undertaken.

Three possible approaches were considered to modify the melting point based on our previous work with nitro-substituted oxadiazoles: (1) replace one of the nitro groups with amino, (2) replace the 1,2,4-oxadiazole moieties with 1,3,4-oxadiazoles, or (3) change the connectivity points of the 1,2,4-oxadiazole in the backbone. Given the fact that replacement of nitro group with amino would in all likelihood decrease the density and increase the melting point, and incorporating the 1,3,4-oxadiazoles into the structure would be synthetically challenging method, method (3) seemed the most attractive. We anticipated that changing the connectivity of 1,2,4-oxadiazole ring within the molecule would change the electron distribution in the molecule, causing different crystal lattice energy and leading to a different melting point. [24] Thus, in the envisaged molecule, **LLM-210**, the pendant 1,2,4-

oxadiazole rings connect to the central 1,2,5-oxadiazole at position-5, instead of that at position-3 as in **LLM-205** (Figure 1).

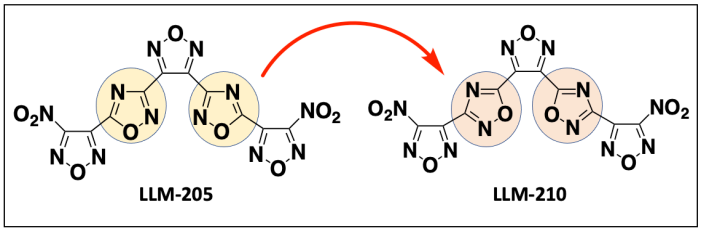

Figure 1. Modification of **LLM-205** by changing the connectivity of 1,2,4-oxadiaozle ring trying to adjust the melting point.

The melting point of an organic compound is difficult to be accurately predicted, but it has been reported that the measurement of the cohesive energy (E_{cov}) of a molecule can indicate trends in melting point predictions for structurally similar molecules. Therefore, using **LLM-205** crystal graphic unit cell and envisaged **LLM-210** molecular structure calculations were performed to compute cohesive energy (E_{cov}) for **LLM-205** and **LLM-210** with density function theory (DFT) using PBE exchange-correlation functional as implemented with the CP2K simulation code. Pseudopotentials of the form GTH was used while valance states was described by Gaussian type orbital basis set (TZV2P) with a plane-wave density cutoff of 600 Ry.[25] Grimme's dispersion correction (D3) was applied.[26] These combination has shown to be effective in predicting molecular structures and dynamics for condense phase systems. The calculated cohesive energy (E_{cov}) for **LLM-205** and **LLM-210**:

E_{cov} = -133.3505 kJ/mol (**LLM-205**)
E_{cov} = -128.5107 kJ/mol (**LLM-210**)

The results show that the energy used to break down the crystal lattice for **LLM-210** is slightly less than that used for **LLM-205**, indicating that the melting point of **LLM-210** may be lower than that of **LLM-205**.

Encouraged by the discovery, a retro-synthetic analysis of **LLM-210** suggested a condensation of nitrile **3** with amidoxime (**11**) at elevated temperatures to form the 1,2,4-oxadiazole rings. Unfortunately, nitrile **3** is proved to be volatile, and was found to be difficult to handle under the reaction conditions. Therefore, an alternative intermediate, diester **10**, was selected as the substrate for condensation with amidoxime (**11**) in the presence of 2,4,6-collidine (Scheme 2).

Scheme 2

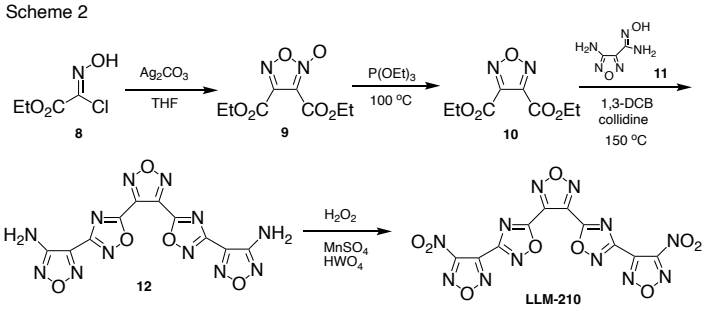

The preparation of **LLM-210** involves multistep reactions. Furoxan **9** was prepared in 80-90% isolated yield from commercially available amidoxime chloride **8** by simply stirring with Ag_2CO_3 in THF at room temperature.[27] The advantage of the coupling reaction with Ag_2CO_3 is that the process does not generate 1,4,2,5-dioxadiazine derivative byproduct resulting from the head-to-tail [3+2]cycloaddition.[28] For the deoxygenation of furoxan to furazan, a common method involves heating furoxans with $P(OEt)_3$ in neat or in an organic solvent. The reaction time and temperature are dependent on the substituent groups on the furoxan ring. For example, dicyanofuroxan (**3**) underwent deoxygenation in refluxing diethyl ether (~40 °C), completed in a few hours, but diester **9** under the same conditions is very slow, requiring overnight to reach 50-70% of the conversion. To accelerate the deoxygenation process, the reaction was carried out at 100-130 °C with no solvent. Under these conditions, the reaction was finished in 1-2 hrs. and the yield of **10** was nearly quantitative. But there is a risk associated with the exothermic reaction. *CAUTION! When $P(OEt)_3$ was added to furoxan diester **9** at room temperature, no reaction could be observed. However, when the reaction mixture was heated and once the deoxygenation initiated, the exothermic reaction become uncontrollable. Therefore, $P(OEt)_3$ must be added to **9** at 100 °C in a rate that the reaction temperature was maintained at 100 -130 °C.*

Diamine **12** was prepared by condensing ester **10** and amidoxime **11** with catalytic amount of collidine at 150 °C. The yield was dependent on the solvent identity and reaction conditions. In our earlier trials, when the condensation was carried out in polar solvents such as anisole, dimethoxybenzene, and *N,N*-dimethylformamide (DMF), giving the yield in < 30%. In non-polar solvents, such as trimethylbenzene or xylene, the sticky precipitate coated on the wall of the flask, making the stirring and heating difficult. However, when 1,3-dichlorobenzene (1,3-DCB) and xylene were combined and the reaction mixture was heated to the designated temperature, the reaction appeared homogeneous throughout the condensing process. Here, xylene was used to azeotrope off water that generated during the condensation reaction. Under these reaction conditions, the yield of diamine **12** was increased to 60-70%.

The oxidization of diamine **12** to **LLM-210** was optimized and improved. Attempts to oxidize **12** with mixture of 70-90% aqueous H_2O_2 in either trifluoroacetic acid (TFA) or in conc. H_2SO_4 with or without catalyst, such as $NaWO_4$, HWO_4, etc. the isolated yield of **LLM-210** was 40-50%, and was accompanied by several unknown by-products as determined by NMR and thin layer chromatography (TLC). Oxidation with 50% aq. H_2O_2, and conc. H_2SO_4 in the ratio of 1:1 (v/v) in the presence of catalytic amounts of HWO_4 at 40-50 °C proved to be the method of choice, significantly improving the yield to 80-90%. But TLC showed that the crude product still contained a major byproduct, which was found in all crude oxidation products and difficult to be removed by recrystallization. The byproduct was isolated and collected from a silica gel column chromatography and eluting with acetone:hexanes (1:3) as a colorless solid, *m.p.* = 163-164 °C. NMR spectroscopy indicated that the byproduct had no protons but 10 inequivalent carbons with chemical shifts at (acetone-d_6) δ166.71, 166.42, 160.38, 160.10, 158.85, 155.31, 143.96, 143.62, 141.65, 140.23 ppm. GC-MS gave a molecular ion peak m/z at

384 (M, 10%), 368 (M-16, 100%). The molecular structure of the byproduct was assigned the cyclic azoxy compound, (4*Z*,12*Z*,16*Z*)-9,12:16,19-di(azeno)tris([1,2,5]oxadiazolo)[3,4-*d*:3',4'-*h*:3",4"*n*][1,12]-dioxa[2,6,7,11]-tetraazacyclo-hexadecine-4-oxide (**14**), forming from an intramolecular condensation between the intermediate oxidation products, hydroxylamino- and nitroso- groups, **13**, as shown in Scheme 3. The final molecular structure was confirmed by single crystal x-ray analysis.

Scheme 3

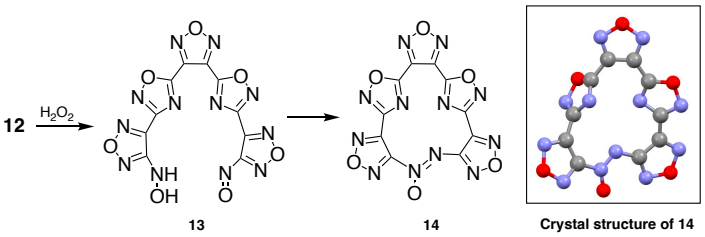

The azoxy compound **14** could not be converted to **LLM-210** with $H_2O_2/H_2SO_4/HWO_4$, indicating that **14** is not an intermediate to **LLM-210**. In the effort to improve the conversion of diamine **12** to **LLM-210** and to reduce the amount of **14**, it was found that Mn(II) is an effective reagent to essentially eliminate the formation of **14**. Under these conditions, **LLLM-210** is the sole isolated product in 80-90% of yield. The role of Mn(II) in the oxidation of amino group to nitro in this synthesis is not completely understood. It is possible that the Mn(II) coordinates with amino- or hydrocylamino- groups during the oxidation, preventing the intramolecular coupling that leads to the formation of **14.**

*Characterization of **LLM-205** and **LLM-210***

The molecule structures of **LLM-205** and **LLM-210** were fully identified by NMR, IR, and single crystal x-ray analysis. In ^{13}C NMR, both molecules have five different carbon resonances with chemical shift at δ 165.5, 160.4, 160 4 (t, J = 19.6 Hz, C-NO_2), 144.8, 139.6 ppm for **LLM-205** and 166.9, 160.6 (t, J = 18.4 Hz, C-NO_2), 159.2, 143.4, 140.9 ppm for **LLM-210**, indicating that both molecules have C_{2v} symmetry in solution.

In the solid state, the conformational structures of **LLM-205** and **LLM-210** are different. For **LLM-205**, the nitro groups on 1,2,5-oxadiazoles unit are turned toward each other, along the axis of the C_{2v} symmetry. However, in **LLM-210** the nitro groups are turned away from the axis of the C2v symmetry (Figure 2).

The packing of **LLM-205** and **LLM-210** in solid state is also different. In **LLM-205** four molecules packed in an orthorhombic crystal system with the space group $P2_12_12_1$ and cell parameters a = 5.6298 Å, b = 13.7709 Å, c = 19.9759 Å. The unit cell volume is 1548.68 $Å^3$ equating to a density (20°C) of 1.807 g/cm^3. **LLM-210** unit cell is monoclinic and composed of two molecules with the space group $P2_1$ and cell parameters a = 7.9054 Å, b = 8.9550 Å, c = 11.5155 Å. The unit cell volume is 766.51 $Å^3$ equating to a density (20°C) of 1.812 g/cm^3. In review of the short contact information from the x-ray analysis, we found that **LLM-205** and **LLM-210** are lacking intramolecular short contact but showing couple of intermolecular interactions at different oxadiazole rings

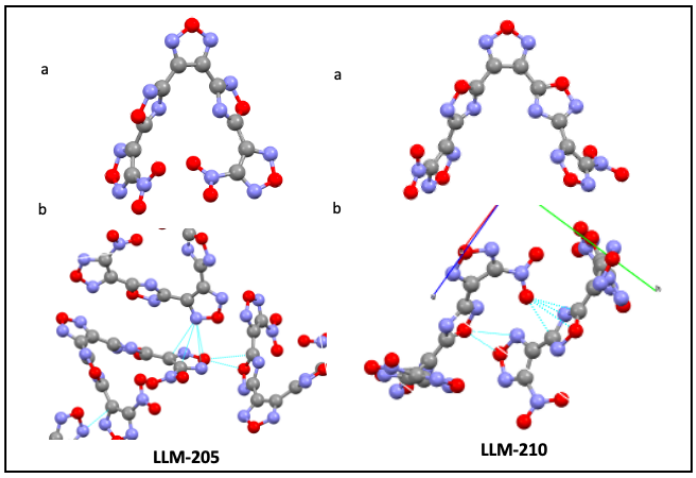

Figure 2. a. Crystal structure of **LLM-205** and **LLM-210**. b. **LLM-205** and **LLM-210** molecules short contact in solid state.

In **LLM-205**, seven pairs of close intermolecular contacts shorter than the sum of the van der Waals radii (3.07 Å for O-N and 3.22 Å for O-C) exist between nitro 1,2,5-oxadiazole ring and the central 1,2,5-oxadiazole unit. In **LLM-210**, six pairs of intermolecular close contacts exist between nitro-1,2,5-oxadiazole and 1,2,4-oxadiazole. A DFT calculation on these two molecules reveal that the central 1,2,5-oxadiazole in **LLM-205** possesses a higher net negative charge than that in **LLM-210** while in **LLM-210** the 1,2,4-oxadiazole rings have relatively higher net negative charges (Figure 3). These results suggest that 1,2,4-oxadiazole ring plays an important role in adjusting the properties of **LLM-205** and **LLM-210**.

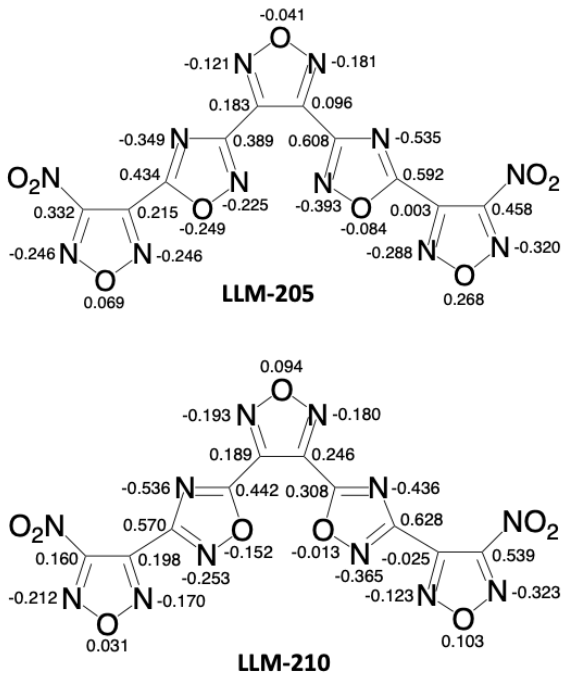

Figure 3. DFT calculations of **LLM-205** and **LLM-210** regarding to the electron charges on heterocyclic rings.

Table 1. Properties of **LLM-205**, **LLM-210** and TNT

Material	m.p. (°C)	ρ [a] (g/cm^3)	T_d [b] (°C)	HoF [c] (kcal/mol)	*IS* [d] (cm)	*FS* [e]	*SS* [f]	CJ [c] (GPa)	DoV [c] (km/s)	Ref
LLM-205	104	1.807	299	123	161	24	no	26.4	8.1	
LLM-210	87	1.812	314	121	167	36	no	26.5	8.1	
TNT	80	1.65	295	-15	100	36	no	20.0	7.2	4,5

a, The density obtained from single crystal x-ray analysis at 20 °C; b, Exotherm peak (heating ramp of 10 °C/min); c, Estimated; d. Impact sensitivity, sensitivity to 2.5 kg drop-weight (HMX standard 32 cm); e, Friction sensitivity, measured with BAM friction sensitivity apparatus; 1/10 attempts @X kg; f, Spark sensitivity, 1.0 J with 510 ohm resistance to model the resistance of a human body.

The small-scale safety and physical properties of **LLM-205** and **LLM-210** were determined and the results are summarized in Table 1 together with the properties of TNT.

The results showed that the similar safety properties of **LLM-205** and **LLM-210** with the exception of the melting point and the friction sensitivity. The melting point of **LLM-210** is 87 °C, lower than that of **LLM-205** in the range of MCEM requirement. The lower melting point of **LLM-210** may be explained from our DFT calculation that the counterpoise cohesive energy of **LLM-210** (-128.5 kJ/mol) is smaller than that of **LLM-205** (-133.4 kJ/mol) which would lead to the decrease melting point. Muravyev *et al*. showed that sensitivity of energetic materials can dependent on many factors for a wide range of CHNOFCl compunds.[29] As LLM-205 and LLM-210 share the same molecular formula but distinct molecular structure it is hypothesize here the interlocking molecular crystal seen in LLM-210 is a contributing factor in lowering the friction sensitivity when compared to LLM-205. (Figure 4) Except the melting point, the friction sensitivity of **LLM-210** is much lower than that of **LLM-205.**

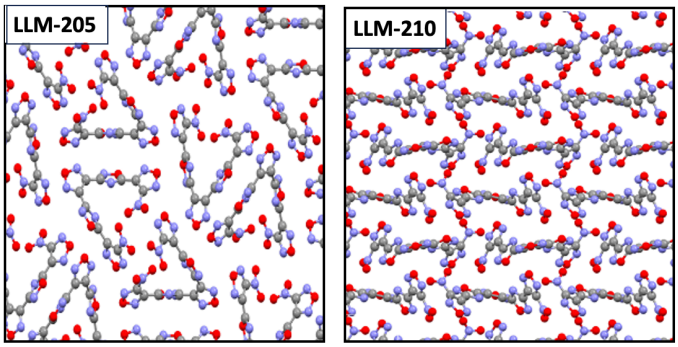

Figure 4. Molecular packing of **LLM-205** and **LLM-210** viewing from a-axis.

LLM-210 is a promising melt-castable energetic material with melting point 87 °C, good impact sensitivity (Dh_{50} =167-176 cm, HMX = 32 cm), high thermal decomposition temperature, (T_d= 314 °C), and good density (ρ = 1.812 g/cm^3). Using the crystal density and estimated heat of formation, the performance of **LLM-210** is better than that of TNT with CJ pressure of 26.5 GPa and detonation of velocity of 8.1 km/s.

Conclusion

LLM-210 composed of five oxadiazole rings arranged as V-type molecular structure was designed, synthesized, and characterized. LLM-210 possesses melting point of 87 °C; high thermal decomposing temperature (T_d = 314 °C); attractive density (ρ = 1.812 g/cm^3); and insensitive to extern stimuli. This makes **LLM-210** as a potential melt-castable energetic material with attributes that rival TNT. **LLM-205**, the isomer of **LLM-210**, shows similar properties with T_d = 299 °C; density, ρ = 1.807 g/cm^3, and also insensitive to extern stimuli except higher melting point (104 °C) and relative higher friction sensitivity in comparison to **LLM-210**. These results together with our earlier reported about the investigation of oxadiazole-based materials,[5, 13, 15-17] indicate that oxadiazole-based material linked by carbon-carbon bonds are thermally stable, insensitive, and high density. It also showed that varying the identity and number of oxadiazole rings is an effective way to modify melting point, sensitivity, and density of a target compound.

Experimental Section

All reagents were purchased from commercial suppliers and used without further purification. Proton and C-13 NMR spectra were acquired on either a Bruker 500 MHz spectrometer (500 and 150 MHz, respectively) or an Anasazi Instruments Eft-90 MHz spectrometer with a Varian magnet (90 and 22.5 MHz, respectively). Proton and C-13 NMR chemical shifts were reported relative to the residual solvent as internal standard, such as, DMSO-d_6 (2.50 ppm for proton and 39.5 ppm for C-13). Infrared spectrum was collected using a Bruker Alpha ZnSe ATR FTIR as thin films.

DSC measurements were performed on a TA instruments DSC Q2000 calibrated to indium and performed at 10 °C/min. An Explosives Research Laboratory type drop-weight apparatus (Drop Hammer) was used to determine the impact sensitivity relative to the primary calibration material HMX (Dh_{50} = 32 cm). The apparatus was equipped with a 2.5 kg weight using 35 ± mg

powder sample in each test. Friction sensitivity was evaluated using a BAM high friction sensitivity tester. Spark sensitivity measured with 510 W resistance meter to model the resistance to a human body.

X-ray crystallography: Crystals were mounted on α MiteGen MicroMesh by using a small amount of Cargille Immersion oil. Data were collected on a Bruker three-circle platform diffractometer equipped with a SMART APEX II CCD detector. The crystals were irradiated by using graphite monochromated MoKα radiation (λ = 0.71073). Data collection was performed, and the unit cell was initially refined by using APEX2 [v2010.3-0]. Data reduction was performed using SAINT [v7.68 A] and XPREP [v2008/2]. Corrections were applied for Lorentz, polarization, and absorption effects by using SADABS [v2008/1]. The structure was solved and refined with the aid of the programs in the SHELXTL-plus [v2008/4] system of programs. The full-matrix least-squares refinement on F2 included atomic coordinates and anisotropic thermal parameters for all non-hydrogen atoms.

Caution! LLM-205 and LLM-210 described in this paper are explosives. They should be handled with caution by qualified personnel only.

4,4'-((1,2,5-oxadiazole-3,4-diyl)bis(1,2,4-oxadiazole-3,5-diyl))-bis(1,2,5-oxadiazol-3-amine) (6)

To a round-bottom flask equipped with magnetic stir bar, dean-stark trap with condenser, and thermometer were added amidoxime (**4**) (12.0g, 64.5 mmol), 3-amino-4-cyano-1,2,5-oxadiazole (**5**) (20 g, 182 mmol), 2,4,6-collidine (2.0 ml, 15.1 mmol), toluene (30 ml) and anisole (80 ml). The mixture was stirred and heated in a pre-heated oil bath at 165 °C for 1.5 hours while collecting azeotropic solution. To the cooled reaction mixture was added water (50 ml) and pentane (100 ml) and stirred for 30 min. The resulting precipitate was collected by suction filtration, washed with water and dried under suction. The crude product was heated and stirred in 500 ml of acetone and filtered to remove any insoluble impurities. The filtrate was concentrated, and the residue was refluxed with water (50 ml). The precipitate was collected by suction filtration when hot and washed with warm water, dried under suction to give diamine **6**, 11.0g (46%). The product can be further purified by silica gel column chromatography (ethyl acetate : methylene chloride, 1:10, R_f = 0.7). mp. 226-228 °C. ^{1}HNMR(acetone-d_6) δ 6.309 (s) ppm. ^{13}CNMR(acetone-d_6) δ 167.4, 158.8, 155.7, 144.0, 134.8 ppm. IR (film) 3466, 3326, 1707, 1641, 1616, 1500, 1135, 976, 953, 769 cm^{-1}. HRMS: m/z = 371.0337 [M-H], corresponding to compound **6**: $C_{10}H_4N_{12}O_5$, calculated: 371.0355 [M-H].

3,4-bis(5-(4-nitro-1,2,5-oxadiazol-3-yl)-1,2,4-oxadiazol-3-yl)-1,2,5-oxadiazole (LLM-205)

Diamine (**6**) (10g, 26.9 mmol) was suspended in 70 ml of trifluoroacetic acid in a water-cooling bath (18 °C). Hydrogen peroxide (70%, 17 ml, ~380 mmol) was added dropwise, controlling the reaction temperature at < 25 °C. The reaction mixture was then stirred at 20 °C overnight to give a clear solution. The reaction mixture was poured into ice-water (400g), stirring at room temperature for 1.0 hour. The precipitate was collected by filtration and washed with water. The crude product was dissolved in methylene chloride (100 ml), the organic phase was washed with water (2X30 ml), dried over magnesium sulfate. After the removal of drying reagent by filtration, the solvent was removed on *vacuo* to yield a white solid. The product was purified by silica gel column chromatography (diethyl ether : hexanes, 1:2, R_f= 0.5) to give **LLM-205**, 4.23g (36%). mp. 104-106 °C. ^{13}CNMR(acetone-d_6) δ 165.5, 160.4, 160.4 (t, *J* = 19.6 Hz, C-NO_2), 144.8, 139.6 ppm. IR (film) 1575, 1358, 1274, 797, 824 cm^{-1}. The product was recrystallized from CH_2Cl_2 and hexane to offer high quality single crystals for x-ray crystallographic analysis.

4,4'-((1,2,5-oxadiazole-3,4-diyl)bis(1,2,4-oxadiazole-5,3-diyl))bis(1,2,5-oxadiazol-3-amine) (10) and 4,4'-((1,2,5-oxadiazole-3,4-diyl)bis(1,2,4-oxadiazole-5,3-diyl))bis(1,2,5-oxadiazol-3-amine) (12)

To a 250 ml of three-necked round bottom flask equipped with an over-head stirrer, thermometer, and a liquid addition funnel, was added triethylphosphite (15.4 g, 93 mmol). The solution was heated in a temperature-controlled oil bath to 100 °C. With stirring, furoxan (**9**) (20.0g, 87 mmol) was added dropwise from the addition funnel (*Caution: Initially, a slow addition is necessary because of the exothermicity of the reaction. The reaction temperature must be closely monitored. If the reaction temperature increases to 110 °C, the addition should be stopped and should not be resumed until the reaction temperature reaches to 100-105°C),* keeping the reaction temperature between 100-130 °C (*If needed, the oil bath temperature may be adjusted to as low as 90 °C to control the reaction temperature but again must be monitored carefully as the reaction temperature should not drop below 100* °C. *Usually, each drop of **9** is added, the reaction temperature increases. If **9** is added and the temperature does not increase, stop the addition, and increase the reaction temperature to 100 °C and then resume addition of **9**. Caution! Never mix triethylphosphite and **9** at room temperature and heat the mix to 100 °C because the reaction will initiate around 100 °C and become uncontrollable*). After the addition was finished, the reaction mixture was heated in the oil bath at 100 °C for further 2.0 hrs. (the reaction progress was monitored by proton NMR).

The liquid addition funnel was replaced with distillation head and the nitrogen gas was introduced slowly. 1,3-Dichlorobenzene (30 ml) was added, following by amidoxime (**11**) (31g, 217 mmol), xylene (10 ml), toluene (10 ml), and collidine (1.0 ml). The oil bath temperature was then increased to 150 °C in a period of 0.5 hr., while collecting/distilling the azeotropic distillate. After ~2.0 hrs. the reaction temperature reached to 145 °C. The heating and stirring was continued for 42 hrs. while collecting/distilling the azeotropic mixture (total 15-16 ml).

The heating was disconnected, and the reaction mixture was allowed to cool to 90 °C. 1,2-dichloroethane (1,2-DCE, 30 ml) was

added carefully with vigorously stirring, followed by 10 ml of hexanes. The stirring was continued, and the reaction temperature was allowed to cool to room temperature (never stop stirring, otherwise the product will be caked, and it is difficult to purify. The best way is to leave it stirring overnight). The precipitate was collected by filtration, washed with 20 ml of 1,2-DCE and 20 ml of hexanes and dried under suction to give 29.7 g of the crude product.

The crude product was refluxed in a mixture of 80 ml of acetone and 40 ml of methanol for 10 minutes. The mixture was allowed to cool to 20-30 °C and the insoluble impurities (~1.5g) was removed by filtration, washed with small amount of acetone. The filtrate was heated to reflux, and 170 ml of water was added at the refluxing temperature (keeping the mixture at the boiling temperature during the addition). After the addition was finished, the mixture was refluxed for further 5 minutes. The precipitate was collected by suction filtration when hot (at the refluxing temperature) and washed with boiling water. The product was dried under suction overnight to give **12** as pale-yellow solid, 16.6 g (51% in two reactions). The material can be further purified by silica gel column chromatography (CH_2Cl_2:Ethyl acetate, 15:1, R_f = 0.5). m.p. 250 °C (decomp.), ^{1}HNMR(DMSO-d_6) δ 6.662 ppm. ^{13}CNMR(DMSO-d_6) δ 165.7, 160.5, 156.0, 143.2, 137.0 ppm. IR (film) 3454, 3343, 1711, 1619, 1075, 944, 766. cm^{-1}. HRMS: m/z = 371.0339 [M-H], corresponding to compound **12**: $C_{10}H_4N_{12}O_5$, calculated: 371.0355 [M-H].

3,4-bis(3-(4-nitro-1,2,5-oxadiazol-3-yl)-1,2,4-oxadiazol-5-yl)-1,2,5-oxadiazole (LLM-210)

To a 500 ml of three-necked round bottom flask equipped with mechanical stirrer, liquid addition funnel, and thermometer, was added 100 ml of H_2O_2 (50%). The solution was cooled in an ice-water cooling bath, H_2SO_4 (95-98%, 100 ml) was added from the liquid addition funnel dropwise slowly with stirring, keeping the reaction temperature between 5-20 °C. After the addition was finished, the reaction mixture was heated to 50 °C and $MnSO_4$ (8.0g, 47 mmol) was added in one portion, followed by HWO_4 (1.0g, 4.0 mmol). Then the liquid addition funnel was replaced with a solid addition funnel. With vigorously stirring, diamine (**12**) (10.0g, 26.9 mmol) was added in portions over a period of 2.0 hrs., keeping the reaction temperature between 50-55 °C. After the addition, the reaction mixture was heated at the temperature for further 1.5 hrs. (monitored by TLC, acetone:hexane,1:3, **12**, R_f = 0.15; **LLM-210**, R_f = 0.35).

The reaction mixture was cooled to room temperature and poured into 400 ml of ice-water. The precipitate was collected by suction filtration, washed with cold water, and dried under suction. The crude product was dissolved in CH_2Cl_2 (20 ml), treated by passing through a short silica gel column (30 g of silica gel, 230-400 Mesh), and eluted with CH_2Cl_2. After removing the solvent, the residue was stirred with 15 ml of diethyl ether for 3 hrs. The colorless solid was collected by filtration and washed with diethyl ether (2X5 ml) to give **LLM-210**, 9.3g (80%). m.p. 86-87 °C. The product was recrystallized from CH_2Cl_2 and hexane to offer high quality single crystal for x-ray crystallographic analysis. ^{13}CNMR (DMSO-d_6) δ 166.9, 160.7 (t, *J*=19.2 Hz), 159.2, 143.4, 140.9 ppm. IR (film) 1562, 1365, 1301, 1115, 989, 823, 752 cm^{-1}.

Author Contributions

Dr. Zhang, Dr. Pagoria, and Dr. DeHope: Chemistry; Dr. Kuo: Computing; Dr. Kerr, and Dr. Parrish: X-ray crystallography

Conflicts of interest

There are no conflicts to declare.

Acknowledgements

The authors would like to thank Jennifer Montgomery for DSC measurements, Stephen Strout for small scale safety tests, and Adele Panasci-Nott for HRMS analysis. Financial support from the Joint DOD/DOE Munitions Technology Program is gratefully acknowledged. This work performed under the auspices of the U.S. Department of Energy by Lawrence Livermore National Laboratory under Contract DE- AC52-07NA27344.

REFERENCES

1. J.-c. Zhang, K. He, D.-w. Zhang, J.-d. Dong, B. Li, Y.-j. Liu, G.-l. Gao and Z.-x. Jiang, *Energ. Mater. Front.*, 2022, **3**, 97-108.
2. Q. Ma, Z. Zhang, W. Yang, W. Li, J. Ju and G. Fan, *Energ. Mater. Front.*, 2021, **2**, 69-85.
3. L. L. Fershtat and N. N. Makhova, *ChemPlusChem*, 2020, **85**, 13-42.
4. D. Frem, *Propellants, Explos., Pyrotech.*, 2023, **48**, e202100312.
5. R. Tsyshevsky, P. Pagoria, M. Zhang, A. Racoveanu, A. DeHope, D. Parrish and M. M. Kuklja, *J. Phys. Chem. C*, 2015, **119**, 3509-3521.
6. S. Gupta, S. S. Goel, H. Siebner, Z. Ronen and G. Ramanathan, *Chemosphere*, 2023, **311**, 137085.
7. S. L. Kober, P. Schaefer, H. Hollert and M. Frohme, *Int. J. Environ. Sci. Technol.*, 2023, **20**, 1399-1410.
8. N. Desai, J. Monapara, A. Jethawa, V. Khedkar and B. Shingate, *Arch. Pharm. (Weinheim, Ger.)*, 2022, **355**, 2200123.
9. U. A. Atmaram and S. M. Roopan, *Appl. Microbiol. Biotechnol.*, 2022, **106**, 3489-3505.
10. Y. Xu, S. Wang, D. Li, P. Wang, Q. Lin and M. Lu, *Org. Process Res. Dev.*, 2023, **27**, 84-89.

11. T. E. Khoranyan, O. V. Serushkina, I. A. Vatsadze, K. Y. Suponitsky, K. A. Monogarov, T. K. Shkineva and I. L. Dalinger, *Russ. Chem. Bull.*, 2022, **71**, 1750-1759.
12. Z. Dong, Z. Wu, Q. Zhang, Y. Xu and G.-P. Lu, *Front. Chem. (Lausanne, Switz.)*, 2022, **10**, 996812.
13. P. Pagoria, *Propellants, Explos., Pyrotech.*, 2016, **41**, 452-469.
14. L. Zhai, F. Bi, H. Huo, Y. Luo, X. Li, S. Chen and B. Wang, *Front. Chem. (Lausanne, Switz.)*, 2019, **7**, 559.
15. R. Tsyshevsky, P. Pagoria, M. Zhang, A. Racoveanu, D. A. Parrish, A. S. Smirnov and M. M. Kuklja, *J. Phys. Chem. C*, 2017, **121**, 23853-23864.
16. P. F. Pagoria, M.-X. Zhang, N. B. Zuckerman, A. J. De Hope and D. A. Parrish, *Chem. Heterocycl. Compd. (N. Y., NY, U. S.)*, 2017, **53**, 760-778.
17. P. Pagoria, M. Zhang, A. Racoveanu, A. DeHope, R. Tsyshevsky and M. M. Kuklja, *Molbank*, 2014, DOI: 10.3390/m824, M824/821.
18. S. Baykov, A. Semenov, M. Tarasenko and V. P. Boyarskiy, *Tetrahedron Lett.*, 2020, **61**, 152403.
19. T. M. Dhameliya, S. J. Chudasma, T. M. Patel and B. P. Dave, *Mol. Diversity*, 2022, **26**, 2967-2980.
20. L. B. Clapp, *Comprehensive Heterocyclic Chemistry, by AR Katritzky and CW Rees, Pergamon Press, New York*, 1984, **6**, 386-391.
21. C. O. Parker, W. D. Emmons, H. A. Rolewicz and K. S. McCallum, *Tetrahedron*, 1962, **17**, 79-87.
22. C. Grundmann, *Chem. Ber.*, 1964, **97**, 3262.
23. D. Fischer, T. M. Klapoetke, M. Reymann, J. Stierstorfer and M. B. R. Voelkl, *New J. Chem.*, 2015, **39**, 1619-1627.
24. M. Kamiya, *Bull. Chem. Soc. Jap.*, 1970, **43**, 3344.
25. S. Goedecker, M. Teter and J. Hutter, *Phys. Rev. B*, 1996, **54**, 1703.
26. S. Grimme, J. Antony, S. Ehrlich and H. Krieg, *J. Chem. Phys.*, 2010, **132**.
27. M.-X. Zhang, A. J. DeHope and P. F. Pagoria, *Org. Process Res. Dev.*, 2019, **23**, 2527-2531.
28. C. H. Lim, T. K. Kim, K. H. Kim, K.-H. Chung and J. S. Kim, *Bull. Korean Chem. Soc.*, 2010, **31**, 1400-1402.
29. N. V. Muravyev, D. B. Meerov, K. A. Monogarov, I. N. Melnikov, E. K. Kosareva, L. L. Fershtat, A. B. Sheremetev, I. L. Dalinger, I. V. Fomenkov and A. N. Pivkina, *Chem. Eng. J. (Amsterdam, Neth.)*, 2021, **421**, 129804.